

tered from various elements at 4.2 Mev are shown in Fig. 4. The interval of inelastic neutron energies taken and the incident neutron energy spreads are indicated in the figures. Figure 5 shows angular distributions obtained with a lead scatterer for various incident energies and energy spreads. In all cases, the distributions are isotropic to within the experimental errors ( $\pm 15\%$ ). These results are in agreement with the predictions of the statistical theory and with the recent results of Thomson et al.<sup>10</sup>

Figure 6 shows the angular distributions of neutrons of energies from 0.5 to 4.0 Mev nonelastically emitted from various elements for an incident neutron energy of 15.2 Mev. No significant deviations from isotropy were observed.

The angular distributions were not corrected for multiple scattering, but due to the fact that the amount of anisotropy was small, the distortions introduced in the distribution by multiple scattering were estimated to be less than about 5%. Cranberg and Levin,<sup>7</sup> as well

as Landon et al.,<sup>9</sup> have made measurements to test this assumption, and they have found that the error introduced by multiple scattering was negligible.

#### IV. CONCLUSION

From the data in the energy region from 3.7 to 4.7 Mev we conclude that, for these energies and for the elements studied, the upper limit for any anisotropy due to direct interaction is 15%.

For incident neutrons of 15.2 Mev, our results also show that the low-energy neutrons (0.5 to 4 Mev) from nonelastic scattering result from compound nucleus formation, in agreement with the results of O'Neill<sup>2</sup> and of Rosen and Stewart.<sup>3</sup>

#### ACKNOWLEDGMENTS

We wish to thank Professor T. W. Bonner, Professor B. B. Kinsey, and Dr. L. Cranberg for their advice and criticisms, and the Texas Nuclear Corporation staff for their help and cooperation.

### Survey of (*p,d*) Reactions at 22 Mev

C. D. GOODMAN AND J. B. BALL  
Oak Ridge National Laboratory,\* Oak Ridge, Tennessee  
(Received December 11, 1959)

Energy spectra of deuterons from (*p,d*) reactions on medium and heavy weight elements were surveyed. The experimental method of particle identification is described. The spectra show gross structure indicative of strong selection rules. The gross structure can be correlated with nuclear shell structure, and the levels which are most strongly excited are those which have the same shell configurations as the target with one neutron missing. Angular distributions confirm the shell assignments. This leads to a picture of the reaction mechanism for (*p,d*) reactions in which the incoming proton interacts principally with a single neutron rather than with the nucleus as a whole.

#### INTRODUCTION

A PREVIOUS study of (*p,d*) reactions with 22-Mev protons showed striking similarities among the deuteron spectra from lead isotopes and bismuth.<sup>1</sup> A survey of (*p,d*) spectra from various elements showed that the shapes of the spectra could not be interpreted as being due to the product of a level density and a Coulomb-barrier penetration function; the intensity of deuterons falls off with decreasing energy well above the Coulomb barrier.<sup>2</sup> In the survey, however, the resolution was not sufficient to show detailed structure.

The present work was undertaken to explore the structure of deuteron spectra from (*p,d*) reactions and to look for element-to-element regularities in the structure of the kind suggested in reference 1.

\* Operated for the U. S. Atomic Energy Commission by Union Carbide Corporation.

<sup>1</sup> B. L. Cohen and S. W. Mosko, Phys. Rev. **106**, 995 (1957).

<sup>2</sup> B. L. Cohen and A. G. Rubin, Phys. Rev. **114**, 1143 (1959).

#### APPARATUS

The proton source is the external beam of the Oak Ridge National Laboratory 86-inch cyclotron which provides 22.2-Mev protons magnetically analyzed by a 15-deg bending magnet. The protons strike a target in the center of a 24-in. diam scattering chamber and stop on a carbon block in a Faraday cup attached to a direct-current integrator. A proportional-counter-scintillation-counter telescope similar to one previously described<sup>3</sup> is mounted on the continuously rotatable upper part of the scattering chamber. The proportional counter is cylindrical with the particle path on the axis and a 0.001-in. tungsten anode wire displaced from and parallel to the axis. The windows are 2.8 mg/cm<sup>2</sup> full hard aluminum foils sealed against neoprene O rings. The window-to-window distance is approximately 10 cm.

<sup>3</sup> C. D. Goodman and J. L. Need, Phys. Rev. **110**, 676 (1958).

The scintillation crystal is NaI(Tl) canned in an airtight mount.<sup>4</sup>

The proportional counter is usually filled to 1½ atmospheres with a gas mixture consisting of 90% argon and 10% methane. In some instances, when only high-energy deuterons are being counted, the gas pressure is increased to two atmospheres to enhance the discrimination between protons and deuterons.

The pulses from the two counters are amplified in doubly differentiating (DD2) amplifiers<sup>5</sup> and fed to a pulse-multiplier circuit, the output of which is of the form,

$$P = (E + k\Delta E + E_0)(\Delta E),$$

where  $E$  is the pulse height from the scintillation counter,  $\Delta E$  is the pulse height from the proportional counter, and  $k$  and  $E_0$  are adjustable constants. The

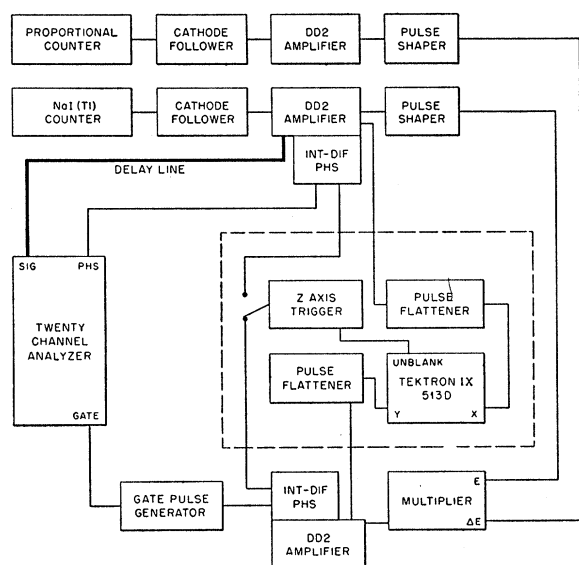


FIG. 1. Block diagram of electronic circuitry.

multiplication is performed with the use of two Raytheon QK329 analog square law tubes, in a circuit similar in logic to one designed by Briscoe.<sup>6</sup>

Figure 1 shows a block diagram of the system. The pulse shapers preceding the multiplier remove the negative swings of the amplifier output which would otherwise appear as a positive output from the squaring tubes, since they perform four quadrant squaring. The steep falling edge of the pulse, characteristic of the output of the DD2 amplifier is maintained. The integral-differential pulse-height selectors are of Fairstein's design<sup>7</sup> in which the output pulse occurs on the falling edge of the input pulse. This feature minimizes the time

<sup>4</sup> C. D. Goodman and J. L. Need, Oak Ridge National Laboratory Report ORNL No.-2066 (unpublished).

<sup>5</sup> E. Fairstein, Rev. Sci. Instr. 27, 475 (1956).

<sup>6</sup> W. L. Briscoe, Rev. Sci. Instr. 29, 401 (1958).

<sup>7</sup> E. Fairstein, Rev. Sci. Instr. 27, 549 (1956).

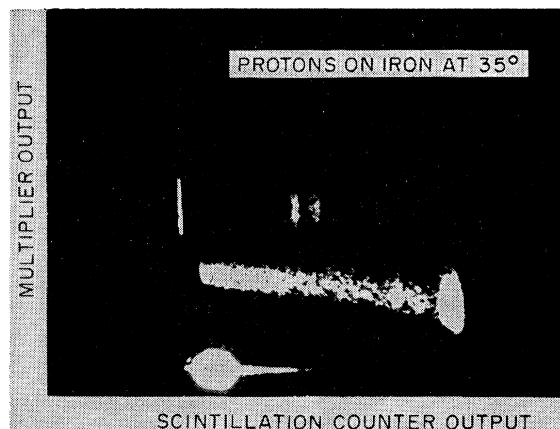


FIG. 2. Time exposure of oscilloscope display. The vertical line at the left represents the gating band chosen for counting deuterons. The horizontal line at the bottom and the flare around it result from gamma-ray pulses from the scintillation counter. The long band is due to protons, and the spots to the right of the vertical mark are due to deuterons.

jitter in the system. The circuit was modified to give separate control of the top and bottom of the slit. Such an analyzer on the multiplier output is used to gate a twenty-channel pulse-height analyzer which records the deuteron energy spectrum. The system shown within the dotted lines is a system for displaying the multiplier output vs energy on an oscilloscope and is identical to the system used previously at this Laboratory.<sup>3</sup> Figure 2 shows a time exposure of the oscilloscope display, and Fig. 3 shows the corresponding pulse-height spectrum from the multiplier for the entire energy band accepted

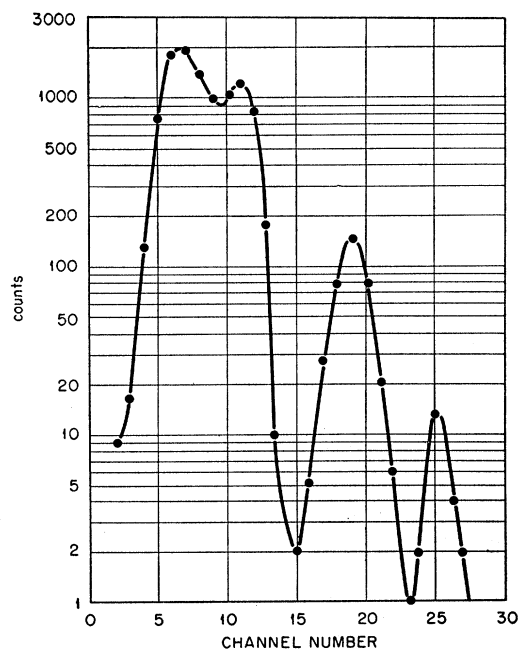


FIG. 3. Pulse-height spectrum from multiplier taken simultaneously with the picture of Fig. 2. Protons on iron at 35°.

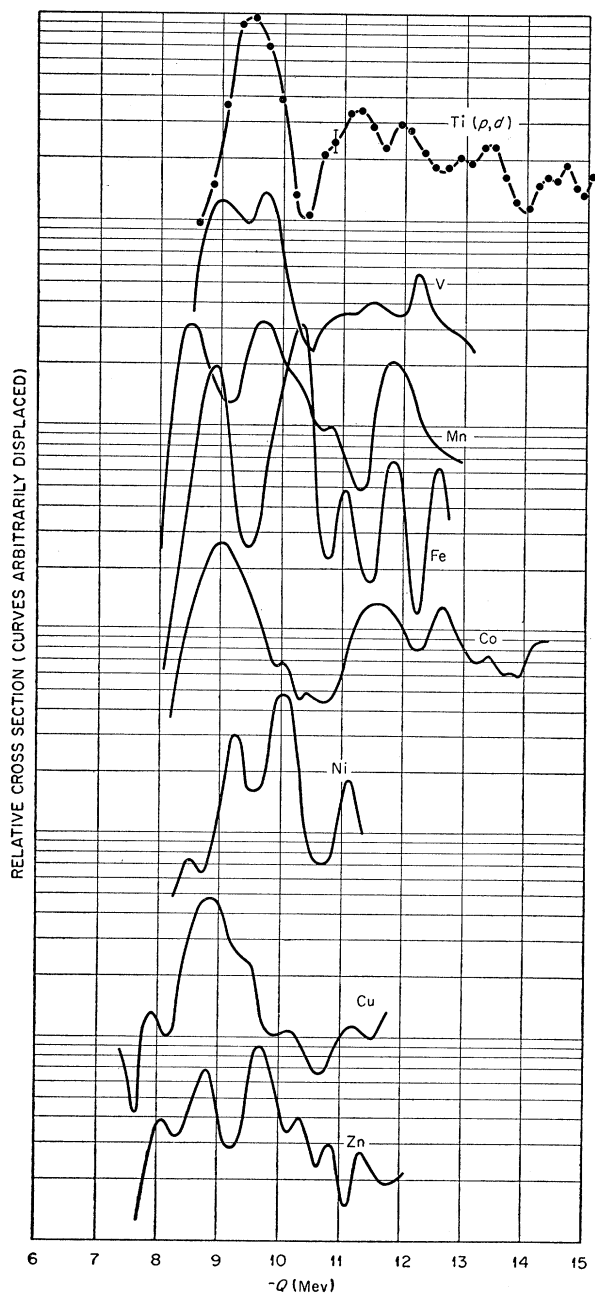


FIG. 4. Typical spectra of deuterons from proton bombardment of the targets indicated.

by the system. The lowest pulse-height group corresponds to protons, the second to deuterons, and the third to tritons. The proton peak is double because the multiplier parameters are adjusted to make the very intense peak due to elastically scattered protons come to a lower pulse height than the rest of the proton distribution. This condition minimizes the counting of elastically scattered protons within the deuteron gating band.

TABLE I. Isotopic analyses of Zr targets.

Major isotope	Atomic percent				
	Zr <sup>90</sup>	Zr <sup>91</sup>	Zr <sup>92</sup>	Zr <sup>94</sup>	Zr <sup>96</sup>
90	98.66	0.768	0.344	0.183	0.041
91	6.91	86.89	5.28	0.816	0.102
92	2.00	1.23	95.38	1.27	0.124

All targets except yttrium and the separated isotopes of zirconium were thin metal foils of natural isotopic abundances. The Zr<sup>90</sup>, Zr<sup>91</sup>, and Zr<sup>92</sup> targets were prepared from enriched isotopes in the form of ZrO<sub>2</sub>. The oxide was suspended in polystyrene dissolved in xylene and poured in a cylinder placed over a piece of 0.0005-in. thick Mylar. The suspension was allowed to settle and most of the xylene was decanted off. The remainder was allowed to dry and the polystyrene served as a binder. The isotopic abundances in the enriched targets are given in Table I.

#### RESULTS AND DISCUSSION

Figures 4, 5, and 6 show a survey of deuteron spectra from several targets of various atomic weights taken at 45 deg with respect to the beam axis. The spectra are plotted as counting rate per Mev vs  $Q$  of the reaction, where  $Q$  is defined in the usual manner as the center-of-mass kinetic energy of the final system minus the center-of-mass kinetic energy of the initial system. Due to uncertainties in the target thicknesses and beam energy, the  $Q$  values may be in error by as much as 0.5 Mev. The reduction of data from the output of the 20-channel

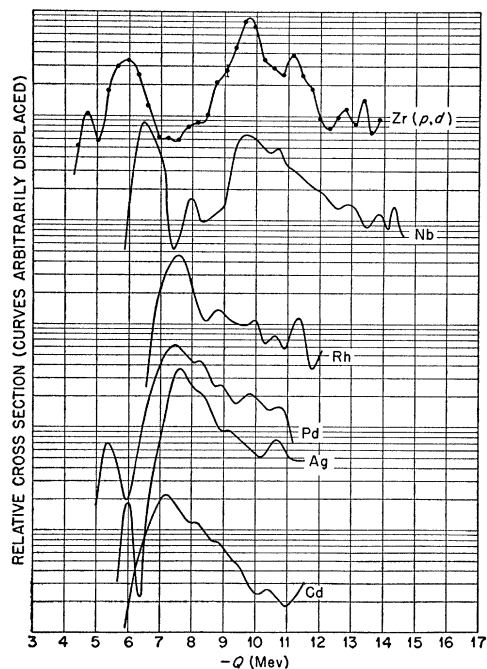


FIG. 5. Typical spectra of deuterons from proton bombardment of the targets indicated.

analyzer was performed on an IBM 704 computer with a data-analysis code called CONDAC I.<sup>8</sup> This code takes into account the energy loss of the particles in the absorber between the target and the scintillation crystal and also performs the solid angle transformation from the laboratory system to the center-of-mass system.

Spectra for Ti, V, Rh, Cd, and Au were also obtained with 19-Mev protons by degrading the cyclotron beam with an aluminum absorber. The analyzed spectra show peaks at the same values of  $Q$  as the 22.2-Mev spectra. This indicates that the deuteron energy is not an important parameter in the gross structure.

Gross structure in the spectra of Figs. 4, 5, and 6 is apparent and there is a hint of element-to-element regularities. The systematics of this gross structure suggests a model for the  $(p, d)$  reaction at these energies based on the following three assumptions: (1) The  $(p, d)$  reaction takes place by a direct interaction; in particu-

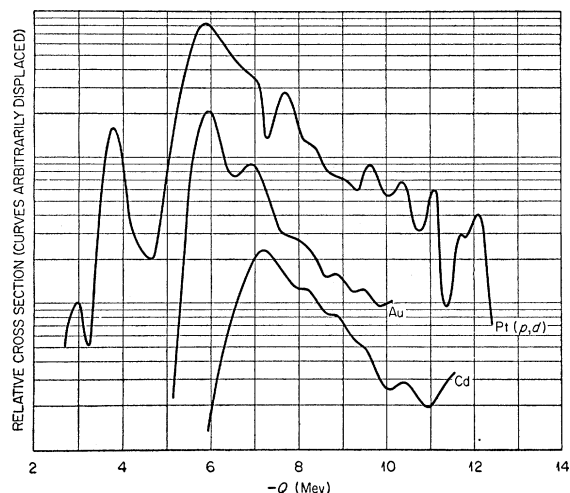


FIG. 6. Typical spectra of deuterons from proton bombardment of the targets indicated.

lar, the incident proton "picks up" a neutron from the nucleus. (2) The shell model provides a good representation of the initial and final states. (3) The interaction of the proton is principally with the neutron which it picks up so that the configuration of the rest of the target nucleus remains unchanged.

To test the validity of this picture,  $(p, d)$  spectra were obtained for the nuclides  $Y^{89}$ ,  $Zr^{90}$ ,  $Zr^{91}$ ,  $Zr^{92}$ , and  $Nb^{93}$ . These targets span the region of the closed neutron shell at  $N=50$  which provides a large gap in the single particle levels that should be evidenced in the deuteron spectra. The deuteron spectra from these targets, taken at 30 deg, is shown in Fig. 7.

The similarity between these spectra is quite striking and in good agreement with the proposed mechanism. The neutron single-particle levels in the region  $N=50$

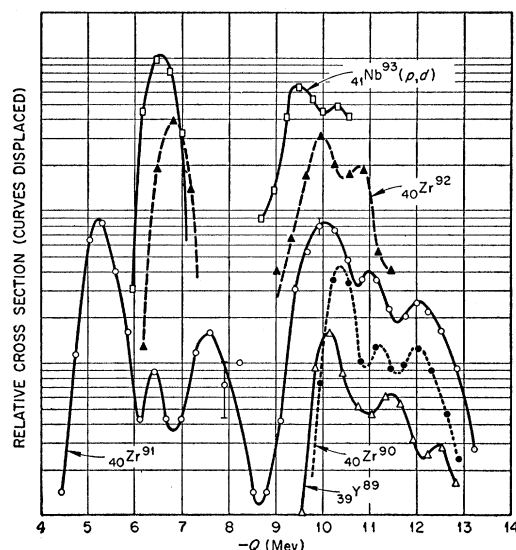


FIG. 7. Spectra of deuterons from proton bombardment of separated zirconium isotopes, yttrium, and niobium. A peak appears near  $Q=-8$  for all these targets but has been omitted in this drawing except for the  $Zr^{91}$  target. The peak is apparently due to nitrogen on the target.

are shown in Fig. 8.<sup>9</sup>  $Y^{89}$  and  $Zr^{90}$  each has fifty neutrons which is a closed major shell. The broad triple peak observed for these elements is attributed to picking up neutrons from the  $g_{9/2}$  level and other nearby levels.  $Zr^{91}$  has 51 neutrons and hence one neutron beyond the closed shell of 50. The broad triple structure observed for  $Y^{89}$  and  $Zr^{90}$  is again seen and is attributed to picking up a neutron from the same levels as before. The extra peak at  $Q \approx -5$  Mev is attributed to picking up the neutron from the  $d_{5/2}$  level. This same argument is easily

$$g_{7/2} \text{ ————— (64)}$$

$$d_{5/2} \text{ ————— (56)}$$

$$g_{9/2} \text{ ————— (50)}$$

$$p_{1/2} \text{ ————— (40)}$$

$$f_{5/2} \text{ ————— (38)}$$

$$p_{3/2} \text{ ————— (32)}$$

$$f_{7/2} \text{ ————— (28)}$$

FIG. 8. Order of shell model states for neutrons (reference 9).

<sup>8</sup> The CONDAC I code was prepared by Mr. B. D. Williams. Copies may be obtained by writing the authors.

<sup>9</sup> M. G. Mayer and J. H. D. Jensen, *Elementary Theory of Nuclear Shell Structure* (John Wiley & Sons, New York, 1955).

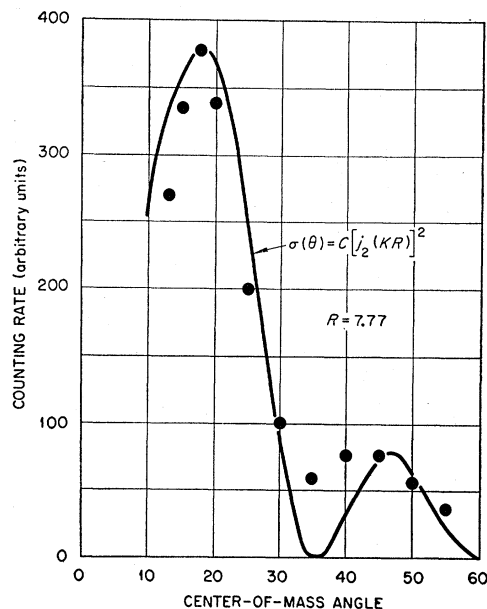


FIG. 9. Angular distribution of the deuteron group from  $Zr^{91}(p,d)Zr^{90}$  to the ground state of  $Zr^{90}$ .

extended to the  $Zr^{92}$  and  $Nb^{93}$  targets where a pair of neutrons are found beyond the closed shell. A peak near  $Q = -8$  appears on all the spectra of Fig. 7 but has been omitted except for  $Zr^{91}$ . This is apparently due to nitrogen on the targets; an enhanced peak in that position was obtained by heating a niobium foil in a nitrogen atmosphere before using it as a target.

An examination of the curves shows that the peak corresponding to removal of the neutron from the pair beyond the closed shell is shifted in energy by about 1.5 Mev from the position of the peak for picking up the single neutron beyond the closed shell in  $Zr^{91}$ . This energy difference is thus the pairing energy for the  $d_{3/2}$  level.

If this interpretation is correct, the angular distributions of the peaks should be characteristic of the orbital angular momentum of the picked-up neutron.<sup>10</sup> An angular distribution for the peak in the  $Zr^{91}$  spectrum at approximately  $Q = -5$  Mev is shown in Fig. 9. The solid line is the spherical Bessel function  $[j_l(Qr)]^2$  which is a simple approximation of the theoretical angular distribution rather than the full expression of the Butler theory involving a Wronskian and a form factor. Employment of the simple square of the Bessel function approximation requires the use of a somewhat large nuclear radius but remains definitive enough to enable the selection of the proper  $l$  value for the pick up. This is amplified below. In the case of Fig. 9 the fit is for  $l = 2$  with a value of  $R = 7.77$  fermis. The known spin of the  $Zr^{91}$  ground state is  $5/2$ , and the shell-model assignment of the odd neutron is  $d_{3/2}$ . Thus the pickup of the odd neutron of  $Zr^{91}$  leaving the  $0^+$  ground state of  $Zr^{90}$  would

<sup>10</sup> S. T. Butler, Phys. Rev. **106**, 272 (1957).

correspond to an  $l = 2$  transition. That the observed peak corresponds to this transition agrees with the angular distribution and the  $Q$  value as obtained from mass data.<sup>11</sup>

If one accepts the interpretation of  $(p,d)$  reactions proposed here, the  $(p,d)$  reaction becomes a very convenient tool for examining the position and properties of filled neutron states. A good example of this is the case of  $Zr^{92}$ . It is probable that the  $d_{3/2}$  and  $g_{7/2}$  levels for neutrons lie quite close together (in fact, for protons the  $g_{7/2}$  fills first). With a pair of neutrons beyond the closed shell,  $Zr^{92}$  has a ground-state spin of  $0^+$ . It is not apparent whether the two neutrons are paired in the  $d_{3/2}$  level or if the additional pairing energy of the  $g$  state will cause them to pair in the  $g_{7/2}$  level.

The angular distribution for the deuteron peak leading to the ground state of  $Zr^{91}$  is almost identical with that of Fig. 9. This says that it is also an  $l = 2$  transition, and the two neutrons beyond the closed shell at 50 pair in the  $d_{3/2}$  level.

In the case discussed above, identification of the proper  $l$  values for the transitions has been made using only the square of the spherical Bessel function. This results in a somewhat large value of the nuclear radius parameter  $r_0$ . For the case of  $Zr^{91}$ , the spherical Bessel fit yields an  $r_0 = 1.7 \times 10^{-13}$  cm. Fitting the first maximum with the more complete Wronskian form of the Butler theory yields a nuclear interaction radius which makes  $r_0 = 1.3 \times 10^{-13}$  cm.<sup>12</sup> It is felt that for identification of  $l$  values, the ease in calculating the simple Bessel function makes it preferable to the Wronskian form.

The broad triple peak occurring in the  $Y^{89}$  and  $Zr^{90}$  spectra suggests that there are three single-particle levels lying near each other at the closed neutron shell of  $N = 50$ . Inability to resolve these peaks adequately with the present system makes identification of the levels uncertain.

For general survey work using the  $(p,d)$  reaction in the identification of single-particle levels, a system with sufficient resolution to define individual levels is required. In the case of zirconium isotopes, the target thickness was the limiting factor, and an effort is being made to prepare thin, uniform targets of the zirconium isotopes. A magnetic analysis system is being set up which should improve the energy resolution over that which is represented in the present work.

#### ACKNOWLEDGMENTS

The authors wish to acknowledge the valuable assistance of E. L. Olson with the electronic circuitry, F. A. DiCarlo and C. L. Viar for cyclotron operation and for assistance in data taking, and R. S. Livingston for his support and encouragement of the experimental program.

<sup>11</sup> A. H. Wapstra, Physica **21**, 367 (1955).

<sup>12</sup> The numerical value was obtained with the aid of the table: C. R. Lubitz, "Numerical Table of Butler-Born Approximation Stripping Cross Sections," University of Michigan (1957) (unpublished).

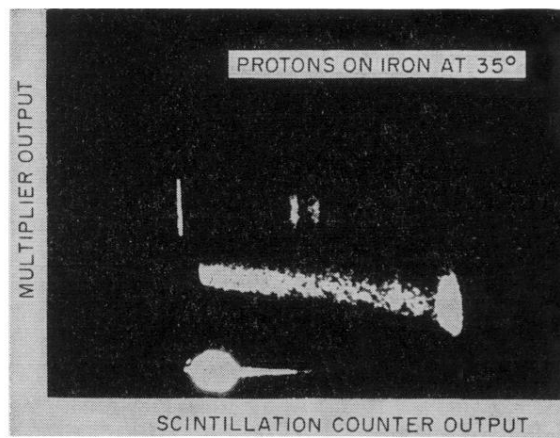


FIG. 2. Time exposure of oscilloscope display. The vertical line at the left represents the gating band chosen for counting deuterons. The horizontal line at the bottom and the flare around it result from gamma-ray pulses from the scintillation counter. The long band is due to protons, and the spots to the right of the vertical mark are due to deuterons.